Earth and Planetary Science Letters 451 (2016) 31–40

Contents lists available at ScienceDirect

Earth and Planetary Science Letters

www.elsevier.com/locate/epsl

Calcium isotope constraints on the marine carbon cycle and $CaCO_3$ deposition during the late Silurian (Ludfordian) positive $\delta^{13}C$ excursion

Juraj Farkaš [a,b,*], Jiří Frýda [c], Chris Holmden [d]

[a] Department of Geochemistry, Czech Geological Survey, Geologická 6, 152 00 Prague 5, Czech Republic
[b] Department of Earth Sciences, University of Adelaide, North Terrace, Adelaide, SA 5005, Australia
[c] Department of Environmental Geosciences, Czech University of Life Sciences, Kamýcká 129, 165 21 Prague 6, Czech Republic
[d] Saskatchewan Isotope Laboratory, Department of Geological Sciences, University of Saskatchewan, 114 Science Place, Saskatoon, SK S7N 5E2, Canada

ARTICLE INFO

Article history:
Received 13 January 2016
Received in revised form 15 May 2016
Accepted 22 June 2016
Available online 21 July 2016
Editor: D. Vance

Keywords:
calcium
isotopes
carbon
cycle
Silurian
ocean

ABSTRACT

This study investigates calcium isotope variations ($\delta^{44/40}Ca$) in late Silurian marine carbonates deposited in the Prague Basin (Czech Republic), which records one of the largest positive carbon isotope excursion (CIE) of the entire Phanerozoic, the mid-Ludfordian CIE, which is associated with major climatic changes (abrupt cooling) and global sea-level fluctuations. Our results show that during the onset of the CIE, when $\delta^{13}C$ increases rapidly from ~0‰ to ~8.5‰, $\delta^{44/40}Ca$ remains constant at about 0.3 ± 0.1‰ (relative to NIST 915a), while $^{87}Sr/^{86}Sr$ in well-preserved carbonates are consistent with a typical Ludfordian seawater composition (ranging from ~0.70865 to ~0.70875). Such decoupling between $\delta^{13}C$ and $\delta^{44/40}Ca$ trends during the onset of the CIE is consistent with the expected order-of-magnitude difference in the residence times of Ca (~10^6 yr) and C (~10^5 yr) in the open ocean, suggesting that the mid-Ludfordian CIE was caused by processes where the biogeochemical pathways of C and Ca in seawater were mechanistically decoupled. These processes may include: (i) near shore methanogenesis and photosynthesis, (ii) changes in oceanic circulation and stratification, and/or (iii) increased production and burial of organic C in the global ocean. The latter, however, is unlikely due to the lack of geological evidence for enhanced organic C burial, and also because of unrealistic parameterization of the ocean C cycle needed to generate the observed CIE over the relatively short time interval. In contrast, higher up in the section where $\delta^{13}C$ shifts back to pre-excursion baseline values, there is a correlated shift to higher $\delta^{44/40}Ca$ values. Such coupling of the records of Ca and C isotope changes in this part of the study section is inconsistent with the abovementioned differences in oceanic Ca and C residence times, indicating that the record of $\delta^{44/40}Ca$ changes does not faithfully reflect the evolution of the oceanic Ca reservoir, but rather some local processes in the Prague Basin. These can be related to *restricted elemental/sediment cycling* involving mixing of isotopically distinct Ca sources and carbonate polymorphs (calcite vs. aragonite), and/or possible *kinetic Ca isotope effects* due to changes in the rate of marine carbonate formation. Evidence supporting the 'kinetic' effect in the studied mid-Ludfordian carbonates is indicated by correlated $\delta^{44/40}Ca$ and Sr-concentration data ($r_s = -0.76$, $p < 0.001$, $n = 41$) yielding a slope of −0.00097, which is indistinguishable from the 'kinetic' slope of abiotic calcite precipitation. Kinetic processes are integral to the model of rapid carbonate precipitation recently proposed by Kozłowski (2015), to explain the origin of the mid-Ludfordian CIE, involving intense methanogenesis/photosynthesis in near shore settings coupled with rapid $CaCO_3$ precipitation (i.e., massive whitings events) and eustatically-controlled *carbonate hypersaturation* of seawater. More Ca isotope studies are needed to shed light on the question of whether *kinetics* or *mineralogy* controls the coupled variations in carbonate $\delta^{44/40}Ca$ and $\delta^{13}C$ records observed in this study and other large positive CIEs in geological record.

* Corresponding author at: Department of Earth Sciences, University of Adelaide, North Terrace, Adelaide, SA 5005, Australia.
E-mail address: juraj.farkas@adelaide.edu.au (J. Farkaš).

http://dx.doi.org/10.1016/j.epsl.2016.06.038
0012-821X/

1. Introduction

Stratigraphic records of carbon isotope values ($\delta^{13}C$) in marine sedimentary rocks of Silurian age show a number of positive carbon isotope excursions (CIE), typically associated with severe biological crises, and synchronized paleo-climatic and sea level changes driven by plausible ice sheet advances and retreats in Gondwana (Munnecke et al., 2003; Loydell, 2007; Calner, 2008; Trotter et al., 2016). The most prominent is the late Silurian (mid-Ludfordian) CIE with associated faunal crises, dated at about 424 million years ago, which is documented globally from different paleo-continents (Fig. 1A), including Baltica (Kaljo et al., 1997; Calner, 2008), Gondwana (Australia, Carnic Alps, cf., Talent et al., 1993; Brett et al., 2009; Jeppsson et al., 2012), Laurentia (Barrick et al., 2010), Perunica (Lehnert et al., 2007a, 2007b; Manda et al., 2012), and Avalonia (Loydell and Frýda, 2011). This globally recognized mid-Ludfordian CIE lasted for about 120 000 yrs (Kozłowski and Sobień, 2012) and reached typical magnitudes of up to +9‰ (Fig. 1B, cf. Frýda and Manda, 2013), with few records from very shallow-water settings showing extreme values up to +11‰ (Jeppsson et al., 2012). Overall, the mid-Ludfordian $\delta^{13}C$ event is the largest positive CIE of the entire Phanerozoic (Munnecke et al., 2003) and is predated by two asynchronous faunal crises: the *Lau conodont Bioevent* and *Kozlowskii graptolite Bioevent* (Jeppsson, 1987; Urbanek and Teller, 1997), also associated with a global scale marine regression and climate cooling (Lehnert et al., 2007a).

The cause of this late Silurian CIE is not yet known. The shear magnitude of this excursion, coupled with the lack of evidence for increased organic carbon deposition in coeval marine sediments (e.g., Frýda and Manda, 2013), argues against increased marine productivity and burial of organic carbon on a global scale as the primary driver of the mid-Ludfordian CIE. The problem is reminiscent of the stratigraphically older (i.e., late Ordovician) Hirnantian CIE, which also recorded extremely positive $\delta^{13}C$ values of up to +7‰ in carbonate sections that are organically lean compared to overlying and underlying sediments (Melchin and Holmden, 2006). Similarly, the Hirnantian CIE is associated with climate cooling, sea level lowstands, and biotic extinctions.

Numerous conceptual models have been offered to explain these early Paleozoic large positive CIEs, stemming from detailed sedimentological investigations of the potential role played by glaciation, sea level, and seawater circulation as factors influencing stratigraphic variation in sedimentary $\delta^{13}C$ values (Jeppsson, 1990; Holmden et al. 1998, 2012a; Bickert et al., 1997; Kump et al., 1999; Panchuk et al., 2006; Melchin and Holmden, 2006; Calner, 2008; LaPorte et al., 2009; Kozłowski and Sobień, 2012; Kozłowski, 2015). Assuming that the positive CIEs indeed reflect primary marine signals, there is also the aspect of *global* vs. *local scale* nature of the inferred C cycle perturbations to consider (cf., Swart, 2008; Swart and Kennedy, 2011), particularly in the Paleozoic where secular records of inferred seawater $\delta^{13}C$ changes are typically reconstructed from the sedimentary deposits of epeiric seas. These shallow marine environments were subject to a variable degree of circulation restrictions with respect to an open ocean (cf., Holmden et al., 1998), which created local conditions that may have influenced the carbonate chemistry of seawater, $CaCO_3$ precipitation rate, mineralogy, and the composition of calcifying biota; all leading to the preservation of spatial and temporal patterns in sedimentary $\delta^{13}C$ records (e.g., Holmden et al., 1998; Immenhauser et al., 2003; Panchuk et al., 2006; Fanton and Holmden, 2007; Swart, 2008; LaPorte et al., 2009).

Thus far, there is no agreed-upon explanation for the origin and primary cause(s) of the mid-Ludfordian CIE, and the available published research presents numerous hypotheses that could be classified based on their *global* vs. *local scale* significance, and the expected degree of coupling between marine C and Ca cycle perturbations. In this context, *global* refers to processes that have the potential to perturb the isotopic composition of the massive oceanic C and Ca reservoirs. Hypotheses offered in this category include: (1) changes in the global ocean stratification and circulation linked to climatic changes (Jeppsson, 1990; Bickert et al., 1997), (2) increased rate of organic carbon burial in the oceans (Kump and Arthur, 1999), (3) increased low latitude weathering of carbonate platforms due to a eustatic marine regression (Kump et al., 1999), (4) changes in the structure of marine primary producers (Calner, 2008; Kozłowski and Sobień, 2012), and/or (5) the burial of authigenic carbonate in anoxic deep ocean sediments (Schrag et al., 2013). In contrast, hypotheses of *local scale* significance refer to the effects of more spatially constrained processes, such as local C and Ca cycling effects in circulation restricted epicontinental seas, vital effects related to changes in marine carbonate producers (i.e., kinetic effects and mineralogical effects), and diagenetic effects. These local-scale processes involve smaller C and Ca reservoirs that respond more quickly, and produce larger isotopic effects, compared to perturbations of the more

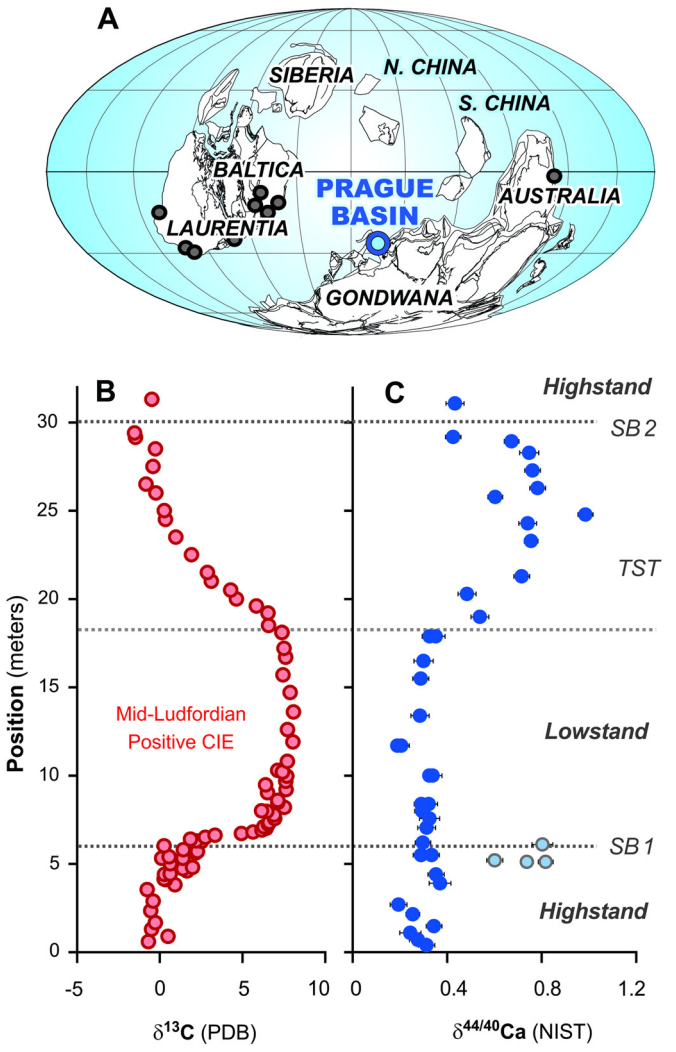

Fig. 1. (**A**) Paleogeographic map showing our study site, i.e., the Prague Basin, and also distribution of other localities (black circles) with published $\delta^{13}C$ records of the mid-Ludfordian carbon isotope excursion (CIE) (modified after Frýda and Manda, 2013; and Torsvik, 2009). (**B**) The $\delta^{13}C$ record across the mid-Ludfordian CIE from the Prague Basin, the Kosov section No. JF195 (data from Frýda and Manda, 2013). (**C**) $\delta^{44/40}Ca$ record across the mid-Ludfordian CIE measured on identical samples that were used for the $\delta^{13}C$ record (see above). Abbreviations used: SB = Sequence Boundary; TST = Transgressive System Track; MFS = Maximum Flooding Surface (after Frýda and Manda, 2013; Kozłowski and Sobień, 2012).

massive oceanic C and Ca reservoirs (Melchin and Holmden, 2006; Fanton and Holmden, 2007; LaPorte et al., 2009; Holmden et al., 2012a). Such local effects can be synchronized by global-scale forcings driven by climate and eustatic sea level changes. Hypotheses offered in this category include: (6) changes in carbonate mineralogy between near and off shore settings (e.g. aragonite vs. calcite which differ in their ^{13}C-enrichment; Swart, 2008), (7) an intense nutrient-driven photosynthesis (Swart, 2008; LaPorte et al., 2009) or methanogenesis (Kozłowski and Sobień, 2012) in shallow water settings, the latter also associated with a possible (8) rapid CO_2 evasion due to massive carbonate precipitation as a result of *carbonate hypersaturation* conditions (Kozłowski, 2015). The nutrient hypothesis was further developed in Holmden et al. (2012b) with the introduction of submarine groundwater discharge (SGD) as an additional means of supplying nutrients to near shore regions of carbonate producing epeiric seas (Holmden et al., 2012a), with the potential to cause shelf gradients in marine δ^{13}C values through near shore increases in primary production (Panchuk et al., 2006; LaPorte et al., 2009).

2. Hypothesis testing

Sea level driven changes in *local scale* elemental cycling within circulation restricted epeiric seas may result in strongly coupled stratigraphic trends in marine δ^{13}C and $\delta^{44/40}$Ca records, as recently shown for the Hirnantian CIE in the Monitor Range section of Nevada (Holmden et al., 2012a). Such coupling between marine δ^{13}C and $\delta^{44/40}$Ca trends is inconsistent with the five to ten times difference in oceanic residence times for Ca and C, implying that the Monitor Range carbonates do not faithfully record the response of the global ocean Ca reservoir. This finding suggests that Ca isotopes might serve as a tool for identifying other instances in geological archives where large CIEs may not faithfully record perturbations of the global ocean–atmosphere C reservoir. In this paper, we apply this test to the mid-Ludfordian CIE recorded in the Prague Basin. The primary goal is to test the plausibility of the above hypotheses (*local* vs. *global*) with the application of Ca isotopes as it is anticipated that certain processes that control the behavior of the marine δ^{13}C proxy might also impact Ca isotopes, while others are expected to have only negligible effect on $\delta^{44/40}$Ca.

Specifically, global scale *changes in ocean circulation and stratification* are not expected to impact marine Ca isotopes, due to the relatively long residence time of Ca in seawater (ca. >1 million years, Ma) compared to a typical mixing time of ~1000 yrs for the global ocean. Similarly, due to a decoupling of biogeochemical pathways of Ca and C in the ocean during *methanogenesis* and/or *photosynthetic fixation* of carbon into organic matter, it is not expected that the purported increase in the production of organic carbon, or methane, would have a direct impact on marine Ca isotopes. It is also not expected that *changes in the structure of marine primary producers*, which could cause shifts in the biologically-controlled C isotope fractionation, would have a major impact on the marine $\delta^{44/40}$Ca proxy unless there was also a concurrent change in the $CaCO_3$ mineralogy (calcite vs. aragonite) of these calcifying organisms (cf., Farkaš et al., 2007; Blättler et al., 2012), and/or their rates of calcification (i.e., kinetic effects; Tang et al., 2008).

On the other hand, *increased weathering of low-latitude shelf carbonates* due to glacio-eustatically controlled regression should lower the $\delta^{44/40}$Ca value of the ocean, while *decreased organic matter weathering in higher latitudes* due to ice covered landscapes (i.e., the carbonate weathering hypothesis of Kump et al., 1999) should increase the δ^{13}C value of seawater. The predicted $\delta^{44/40}$Ca and δ^{13}C shifts may not be synchronous as this will depend on relative magnitudes of Ca and C weathering flux perturbations, and the size of the oceanic Ca and C reservoirs. Moreover, the expected shift to lower seawater $\delta^{44/40}$Ca values might be relatively short-lived as the increased alkalinity flux to oceans from carbonate weathering will eventually lead to increased marine $CaCO_3$ precipitation and carbonate burial. This would drive seawater $\delta^{44/40}$Ca in the opposite direction, i.e., to higher values. Finally, the newly proposed *carbonate hypersaturation* hypothesis (Kozłowski, 2015), invoking an eustatically driven global supersaturation of seawater in near shore settings during the mid-Ludfordian CIE, is expected to be recorded in the coeval marine carbonates as kinetic or rate-controlled Ca isotope effects due to presumably faster and more kinetically-controlled precipitation of marine carbonates (cf., Tang et al., 2008).

3. Materials and methods

3.1. Study sites and samples

Marine carbonates investigated in this study are proximal shelf deposits, sampled from the late Silurian Kopanina Formation at the Kosov Quarry (i.e., section No. JF195), exposed in the Prague Basin (Czech Republic) that represents a small relict of the former and much larger Paleozoic basin (Frýda and Manda, 2013; Lehnert et al., 2007b). Paleomagnetic data indicate that during the Ludfordian period the basin was located approximately 25 to 30 degrees south of the paleo-equator (Fig. 1A), either on the northern margin of Gondwana (i.e., peri-Gondwana) or on an isolated 'microcontinent' called Perunica (Torsvik, 2009). The depositional system of the Prague Basin represents an extensional rift basin that was formed on submerged continental crust inundated by shallow seas, and surrounded by deeper (i.e., hemipelagic) open marine settings (Kříž, 1991). Hence, the studied carbonates consist of a variety of facies including: fine-grained (micritic mudstone, wackestone), coarser crinoidal grainstones (packstone), and laminated calcareous shales (see Appendix, Table A1; Fig. A1). The mid-Ludfordian carbonates investigated in this study are identical with those used in Frýda and Manda (2013) to reconstruct a complete δ^{13}C record of the mid-Ludfordian CIE.

Additional samples represented by tuffitic limestones (i.e., organodetritic carbonates with tuffitic admixture) were collected from base of the Kopanina Formation at the Kosov Quarry with the aim to better constrain the Ca and Sr isotope composition of possible 'volcanic' sources present in the Prague Basin and the analyzed mid-Ludfordian carbonates. Finally, a set of stratigraphically older (i.e., Homerian; upper Wenlock) marine carbonates was also collected from the Kozel Member of the Motol Formation (the section No. 760; Frýda and Frýdova, 2014; and Kozel Syncline section No. 244JF; Frýda and Frýdová, 2016) to identify the isotope signatures of local carbonate sources with the potential to be physically weathered and redeposited in the study setting.

3.2. Elemental and isotope analyses

For the elemental and isotope analysis, we sampled a few milligrams of powder from 'bulk' carbonates, targeting where possible micritic mudstones or wackestones (see Appendix; Tables A1 and A2). The sampling was performed with a micro-drill tool from cut rock fragments or polished slabs. Major and trace element analyses were performed using an ICP AES instrument at the Saskatchewan Research Council Analytical Laboratories in Saskatoon, Canada, with a reproducibility of $\pm 10\%$ (2σ).

For the Ca isotope analyses, homogenized carbonate powders were dissolved in 0.5 N HCl at room temperature until effervescence ceased and the solutions were mixed with a ^{43}Ca–^{42}Ca tracer, i.e., double spike. These spiked samples were then passed through cation-exchange columns containing 3 ml

of Biorad MP-50 resin to purify the Ca fraction from other ions present in carbonate matrix. The Ca isotope analyses were performed by thermal ionization mass spectrometry (TIMS), using a Thermo Fisher Triton instrument located in the Saskatchewan Isotope Laboratory, following the procedures described in Lehn et al. (2013). Data are reported in the delta notation: $\delta^{44/40}Ca = [(^{44}Ca/^{40}Ca_{sample}/^{44}Ca/^{40}Ca_{NIST915a}) - 1] \times 1000$, as per mil (‰) differences relative to NIST 915a standard. The $\delta^{44/40}Ca$ data reported on the 915a scale may be converted to the seawater scale (e.g., IAPSO) by subtracting 1.86. Seawater measured over the course of this study yielded 0.0 ± 0.06‰ ($n = 10$, 2σ). The overall reproducibility of our $\delta^{44/40}Ca$ data based on measurements of seawater and repeated analysis of individual samples is also ~0.06‰ (2σ). Selected carbonate samples were also analyzed for $^{87}Sr/^{86}Sr$ (see Table A1). The Sr was purified using same MP50 columns used for Ca. The $^{87}Sr/^{86}Sr$ measurements were performed by TIMS in static multi-collection mode, and corrected for instrumental mass fractionation using 0.1194 for the ratio of $^{86}Sr/^{88}Sr$. The external reproducibility of $^{87}Sr/^{86}Sr$ analyses is better than ±25 ppm (2σ) based on repeated measurements of samples and the NIST SRM 987 standard yielding analytical errors of ±0.000014 (2σ). Due to the nature of our geochemical datasets, which do not show normally distributed variables, the statistical evaluation of correlation patterns between these variables is based on the Spearman's (r_s), rather than Pearson's, correlation coefficient.

4. Results

A total of 36 relatively pure marine carbonates (i.e., limestones) with mid-Ludfordian ages were selected and analyzed for their $\delta^{44/40}Ca$ values that vary from 0.19 ± 0.04‰ to 0.99 ± 0.03‰ (2σ), thus covering an overall range of ~0.80‰ (see Fig. 1C, and data in Table A1, Appendix), which compares to a range of ~ 8.5‰ for $\delta^{13}C$. In addition, 2 samples of less pure mid-Ludfordian limestones (i.e., tuffitic calcareous shales) gave $\delta^{44/40}Ca$ from 0.89 ± 0.03‰ to 1.00 ± 0.03‰, and a total of 18 carbonates (i.e., organodetritic limestones) with stratigraphically older (i.e., Homerian) ages yielded $\delta^{44/40}Ca$ from 0.51 ± 0.03‰ to 0.82 ± 0.03‰ (see Fig. 2; and data in Table A2 and Fig. A2, in Appendix).

The stratigraphic $\delta^{44/40}Ca$ profile of the mid-Ludfordian carbonates (from 0 to 31 m, see Fig. 1C) displays the following features: (i) a rather constant $\delta^{44/40}Ca$ of about 0.30 ± 0.10‰ during an interval from 0 to 18 m; (ii) followed by a systematic increase to higher $\delta^{44/40}Ca$ values of about 0.80 ± 0.10‰ between 18 to 25 m; and (iii) a subsequent decline to about 0.40 ± 0.05‰ recorded in the upper part (29 to 31 m). Four carbonate samples located in a narrow interval between 5 to 6 m, thus in the vicinity of the sequence boundary (SB), yielded high $\delta^{44/40}Ca$ from 0.60 to 0.82‰ (Fig. 1C, light blue circles), which therefore plot away from the *main* stratigraphic $\delta^{44/40}Ca$ trend (Fig. 1C, dark blue circles). Microscopic analysis of these four samples confirmed that they are from an interval dominated by calcareous/tuffitic shales containing lenses of micritic mudstones and wackestones. However, in general, we observe that micritic mudstones and wackestones are associated with lower $\delta^{44/40}Ca$ values (about 0.3 to 0.4‰), while micritic packstones tend to yield higher $\delta^{44/40}Ca$ of about 0.5 to 0.9‰ (for details see Appendix, Table A1).

The trend in $\delta^{44/40}Ca$ values between 0 and 18 m is relatively constant at 0.30 ± 0.10‰, whereas the $\delta^{13}C$ profile shows an excursion from ~ 0.0‰ to 8.5‰ (Fig. 1B, C), thus indicating that the sedimentary C and Ca isotope records are significantly decoupled over this stratigraphic interval ($r_s = -0.11$, $p = 0.57$, $n = 28$), (see also Fig. A4 (A), in Appendix). In contrast, higher up in the section where the falling limb of the CIE occurs, a strong negative correlation between $\delta^{13}C$ and $\delta^{44/40}Ca$ is observed between 19 and 31 m ($r_s = -0.78$, $p < 0.001$, $n = 15$; see Figs. 1B, C). Finally, the measured $^{87}Sr/^{86}Sr$ ratios of the mid-Ludfordian carbonates vary from 0.70839 to 0.70868 ± 0.00001 (2σ), and $^{87}Sr/^{86}Sr$ of the Homerian samples range from ~0.70781 to 0.70825 ± 0.00001 (see Fig. 2A, Tables A1 and A2). Our results also indicate a general coupling between $^{87}Sr/^{86}Sr$ and $\delta^{44/40}Ca$ that is particularly strong in micritic carbonates from massive carbonate layers, and those with some (but not abundant) tuffitic material mixed into the carbonate sediment (see black and gray circles in Fig. A5 (A), in Appendix).

Overall, the mid-Ludfordian CIE exhibits a stratigraphic pattern that is strongly correlated with the lithofacies record of relative sea-level changes (see Fig. 2D; Frýda and Manda, 2013). Specifically, the lithological data from the Prague Basin indicate the observed stratigraphic rise and fall in $\delta^{13}C$ values closely tracks the regression and subsequent transgression of sea level, respectively (Frýda and Manda, 2013; Lehnert et al., 2007a; but see also alternative sea-level reconstructions in Kozłowski and Sobień, 2012; and Kozłowski, 2015).

5. Discussion

5.1. Strontium isotope constraints on diagenetic history and the marine origin of carbonates

The $^{87}Sr/^{86}Sr$ proxy, which is strictly an isotope tracer of geological and hydrological Sr sources, is applied here to evaluate the role of (i) diagenetic processes, and (ii) the degree of seawater restriction between the Prague Basin and the open ocean during the period of carbonate deposition. The main source of Sr in the studied carbonate should be Ludfordian seawater with $^{87}Sr/^{86}Sr$ ranging from ~0.70865 to ~0.70875 (Cramer et al., 2011). However, continental inputs of Sr from riverine, groundwater and/or aeolian sources could result in a non-marine $^{87}Sr/^{86}Sr$ signature being recorded in the studied carbonates if seawater circulation between an open ocean and the Prague Basin was restricted. Other processes that could be responsible for the non-marine $^{87}Sr/^{86}Sr$ in the studied samples include (i) a post-depositional release of Sr from siliciclastic components (i.e., detrital, tuffitic, aeolian) present in the bulk carbonates, and/or (ii) the input and subsequent incorporation of radiogenic Sr from meteoric waters into the carbonates during later diagenesis. Overall, the studied samples are dominated by relatively pure micritic/bioclastic carbonates (mudstones, wackestones and packstones) with a few occurrences of calcareous tuffitic shales and marls (for details see the sample lithologies in Table A1; and Frýda and Manda, 2013).

Our results show that the typical *open ocean* $^{87}Sr/^{86}Sr$ signatures, characteristic of Ludfordian seawater (~0.70865 to ~0.70875), are present only in fine-grained limestones (micritic mudstones) sampled from the massive carbonate layers between 0 and 19 m in the section (see Fig. 2A, and solid black circles connected with a black line). Thin-bedded and laminated micritic/skeletal limestones yielded lower $^{87}Sr/^{86}Sr$ ratios than Ludfordian seawater (cf., gray circles in Fig. 2A), falling within the expected range of older Gorstian seawater (i.e., ~0.70845 to ~0.70865; Cramer et al., 2011). The least radiogenic $^{87}Sr/^{86}Sr$ ratios (as low as ~0.70835), falling in the range of even older (Homerian) seawater, were measured in coarser grained sediment with evidence of detrital carbonate (e.g., crinoidal debris and shell fragments). These units were deposited near the sequence boundary (SB) where there are also occurrences of thin-layered tuffitic calcareous shale and marl (see open circles in Fig. 2A; from depths ~4 to 8 m). The presence of volcanic Sr from tuffitic materials in the studied carbonates is not surprising considering the existence of the nearby *Kosov* and *Svaty Jan* Volcanic Centres, where repeated eruptions of basalt occurred between the Homerian and late Gorstian (cf., Kříž, 1991).

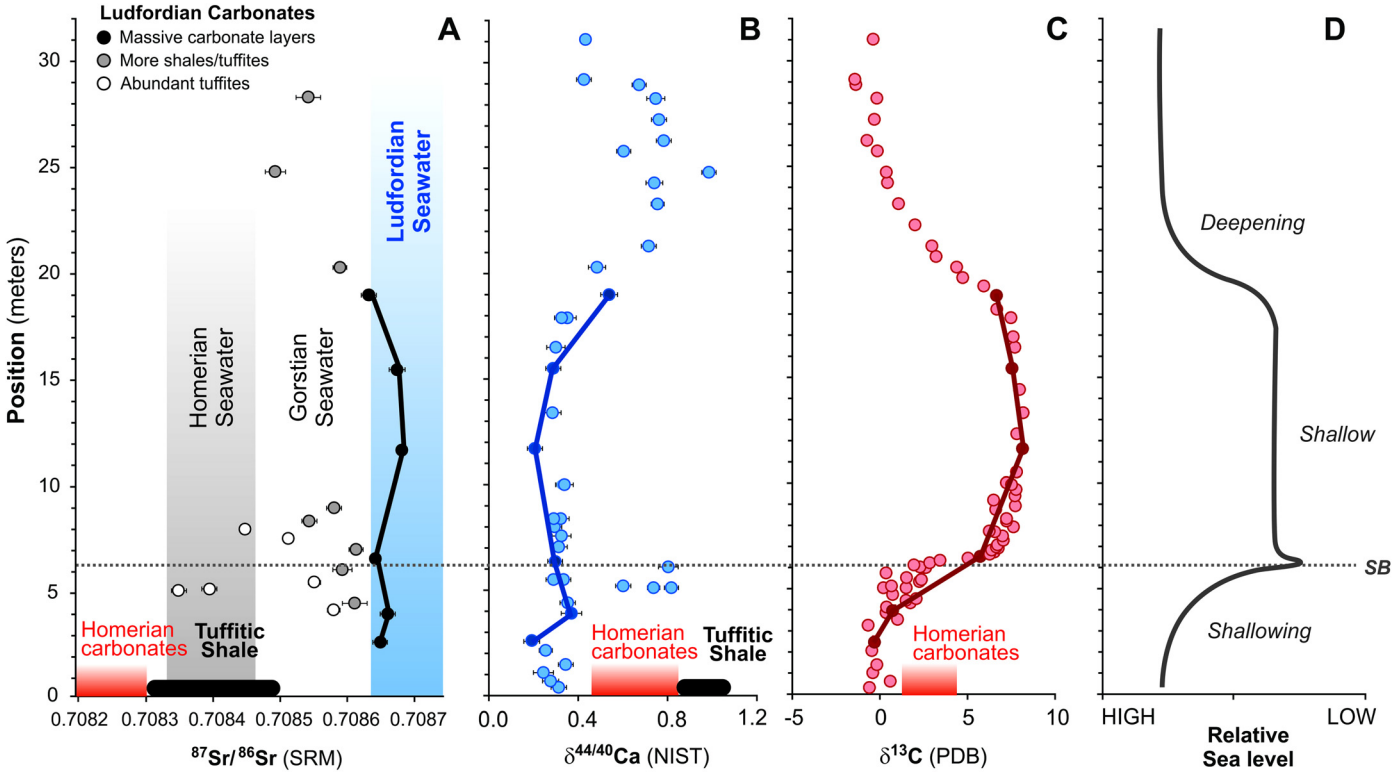

Fig. 2. (**A**) The $^{87}Sr/^{86}Sr$ record of selected mid-Ludfordian carbonates from the Prague Basin, along with a range of $^{87}Sr/^{86}Sr$ expected for the Ludfordian, Gorstain and Homerian seawater (i.e., vertical rectangles; based on Cramer et al., 2011). Black, grey and open circles indicate the identified lithologies and documented tuffite occurrences for these samples (see the legend; based on sedimentological data from Frýda and Manda, 2013). (**B**) The $\delta^{44/40}Ca$ record of the mid-Ludfordian carbonates (i.e., open blue circles), showing also samples that yielded $^{87}Sr/^{86}Sr$ consistent with the Ludfordian seawater (i.e., dark blue circles connected with a solid line). (**C**) The $\delta^{13}C$ record of the mid-Ludfordian carbonates from the Prague Basin (data from Frýda and Manda, 2013). The solid line connects data that were analyzed for $^{87}Sr/^{86}Sr$ and yielded values consistent with the Ludfordian seawater. (**D**) A schematic reconstruction of relative fluctuations in a local sealevel (based on Frýda and Manda, 2013). Black rounded rectangles and red squares indicate, respectively, the measured isotope signatures of tuffitic calcareous shales and Homerian carbonates. Abbreviations used: SB = Sequence Boundary. (For interpretation of the references to color in this figure, the reader is referred to the web version of this article.)

Overall, these associations point to diagenetic processes as being an important factor controlling the $^{87}Sr/^{86}Sr$ pattern of the studies mid-Ludfordian carbonates, suggesting that diagenetic fluids with less radiogenic Sr (due to dissolution of interbedded tuffitic components with basaltic composition), and its later incorporation into the carbonates, were likely responsible for the observed shifts to 'non-marine' Sr isotope ratios recorded through the profile. Nevertheless, it is also possible that detrital carbonates with lower $^{87}Sr/^{86}Sr$ signatures (e.g., Gorstian and Homerian limestones; cf. data in Table A2, and Cramer et al., 2011), eroded from the exposed carbonate platform margins during the sea level lowstand, could be responsible for the observed shifts to less radiogenic $^{87}Sr/^{86}Sr$ ratios, the latter typically associated also with higher $\delta^{44/40}Ca$ values (see Fig. 2A, B; and Fig. A5 (A) in Appendix).

Regardless of the exact mechanism(s) responsible for the *non-marine* $^{87}Sr/^{86}Sr$ signatures observed in some of the mid-Ludfordian carbonates (see Fig. 2A, open and gray circles), it is important to note that the stable Ca and C isotope signatures in marine carbonates are more resistant to diagenetic resetting than $^{87}Sr/^{86}Sr$ (which is a trace-element isotope proxy). Thus, large *water to rock* (W/R) ratios of about 10 000 are required to reset $\delta^{13}C$ and $\delta^{44/40}Ca$ values in marine limestones via post-depositional alteration (i.e., by diagenetic/meteoric fluids), which compares to W/R ratios of only about 100–1000 needed to rest $^{87}Sr/^{86}Sr$ (Banner and Hanson, 1990; Husson et al., 2015). Hence, the finding that certain mid-Ludfordian carbonates are diagenetically altered with respect to their seawater $^{87}Sr/^{86}Sr$ signatures, does not imply that their $\delta^{13}C$ and $\delta^{44/40}Ca$ values are also significantly altered, as these are expected to be more buffered against diagenetic resetting.

Importantly, our results from the least altered samples (i.e., micritic mudstones from massive carbonate layers), which yielded $^{87}Sr/^{86}Sr$ typical of Ludfordian seawater (Fig. 2A; black line), show that in the beginning stages of the mid-Ludfordian CIE when carbonate $\delta^{13}C$ values increase from ~0‰ to ~8.5‰ (see Fig. 2C, blue line), the $\delta^{44/40}Ca$ values remain constant at ~0.3‰ (Fig. 2B, red line). This different behavior suggests that the CIE was produced by process(es) where the biogeochemical pathways of C and Ca in the late Silurian ocean were decoupled on a time scale of tens of thousands of years, which is the estimated duration for the initial rise of the CIE (for details see below; and Kozłowski and Sobień, 2012).

5.2. Relationship between marine Ca and C isotope records: insights from residence times

Estimates based on sediment deposition rates and biostratigraphy (i.e., the thickness-time relation) indicate that the duration of the mid-Ludfordian CIE is of the order of 100 000 yrs (for details see Kozłowski and Sobień, 2012). Specifically, it has been estimated that the initial shift to high $\delta^{13}C$ values at the base of the CIE occurred in ~40 000 yrs in Baltica, and that the peak-interval in the $\delta^{13}C$ excursion lasted about 120 000 yrs (cf., Kozłowski and Sobień, 2012; Kozłowski, 2015).

In order to better understand the origin of the observed Ca and C isotope trends (Figs. 1B, C), and whether they represent *local* or *global* scale Ca and C cycling processes, we need to consider how

the $\delta^{44/40}$Ca and δ^{13}C proxies are expected to behave to perturbations in the ocean Ca and C reservoirs (e.g., Holmden et al., 2012a). The rate of response of an isotope tracer such as $\delta^{44/40}$Ca in the ocean reservoir is dependent on many factors, but primarily on the residence time (τ) of the dissolved Ca^{2+} in seawater, which is defined as:

$$\tau = \frac{M_{(SS)}}{F_{(SS)}} \quad (1)$$

where M represents the total mass of the dissolved Ca^{2+} ions in the ocean under the steady-state (SS) conditions; and $F_{(SS)}$ is the total steady-state input (or output) flux of Ca^{2+}.

Accordingly, the rate of the response (or the decay) of the ocean Ca cycle to a perturbation can be quantified using the following relationship:

$$\delta^{4}Ca_{(T)} = \delta^{44}Ca_{(T0)} \cdot e^{(\lambda T)} \quad (2)$$

where $\delta^{44}Ca_{(T)}$ and $\delta^{44}Ca_{(T0)}$ represent, respectively, the isotope signatures of the oceanic Ca reservoir at the time of interest (T), and during the 'peak' steady-state conditions caused by the perturbation event ($T0$). A parameter λ represents a 'decay constant' that is characteristic for a particular system, and dependent on the residence time (τ) of the tracer, according to:

$$\lambda = \frac{1}{\tau} \quad (3)$$

Thus, knowing the residence times of calcium (Ca^{2+}) and carbon (DIC) in the late Silurian oceans (or rather the anticipated difference in their residence times) one can model the expected response times of Ca and C isotope proxies in the ocean to environmental perturbations associated with the mid-Ludfordian CIE.

Studies of the fluid inclusions of marine evaporites (Horita et al., 2002), and/or results of long-term geochemical models (cf., Mackenzie and Andersson, 2013), indicate that the concentrations of Ca^{2+} and DIC in the late Silurian seawater were both approximately two to three times higher compared to their modern values (Ca^{2+} = 10.2 mmol/kg and DIC = 2.3 mmol/kg). Taking into account the estimated magnitudes of Ca and C input fluxes to Silurian oceans of about ~15 and ~35 Tmols/yr, respectively (Mackenzie and Andersson, 2013), the calculated mean residence times of Ca^{2+} and DIC in Silurian seawater are ~2.5 millions of years (Ma) and ~200 000 yrs, respectively.

Considering these residence times, our calculations (based on Eq. (2)) indicate significantly different recovery (or *settling*) times for perturbations of the marine Ca and C cycles during the mid-Ludfordian event. In general, the calculations show that it takes approximately five residence times (τ) for a particular isotope tracer to return from steady-state 'peak' values (i.e., plateau), back to the 'normal' pre-excursion baseline values once the forcing of such perturbation is removed. It should therefore take approximately 10 times longer to remove a perturbation in $\delta^{44/40}$Ca than a perturbation in δ^{13}C, assuming that both of these proxies record changes in the ocean Ca and C cycles preserved in marine carbonates (Holmden et al., 2012a).

In Fig. 3A and B, respectively, the δ^{13}C and $\delta^{44/40}$Ca data from the upper interval (from 7 to 29 m) are plotted together with the modeled 'response/settling' trajectories of these isotope tracers in the ocean. These are calculated for different scenarios of the Ca and C residence times in the oceans, specifically 20 000, 100 000, and 1000 000 yrs (see the curves in Fig. 3A, B). Note that the isotope data and model results are plotted against a time scale covering an interval of 200 000 yrs, which approximates the anticipated duration of the mid-Ludfordian CIE event (i.e., the heavy plateau interval and the falling limb), (Kozłowski and Sobień, 2012). Our modeling results show that it is impossible to generate a change

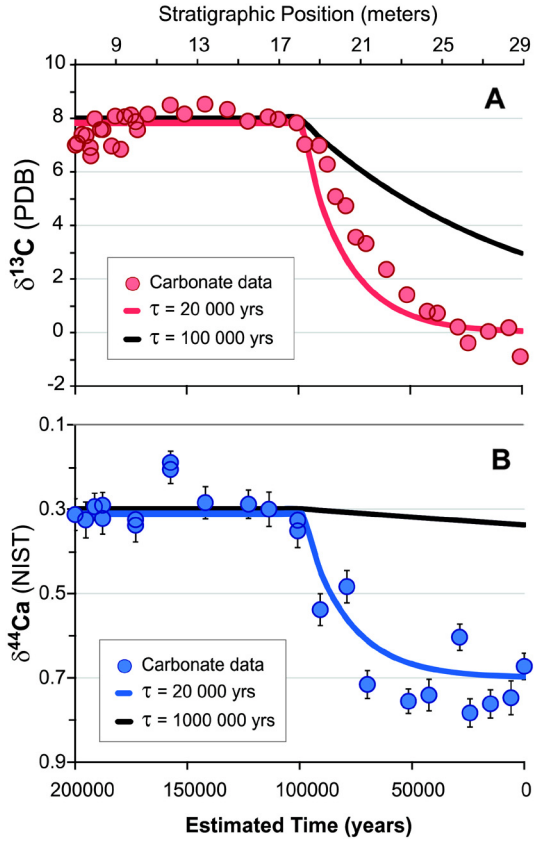

Fig. 3. (**A**) The δ^{13}C record showing a section of the mid-Ludfordian CIE (Kosov, the Prague Basin) for an interval from 7 to 29 meters (m), together with the modeled 'response curves' for the marine δ^{13}C proxy based on different residence times (τ) of carbon in the late Silurian oceans, which are set up at hypothetical values of 20 000 and 100 000 yrs. (**B**) The δ^{44}Ca record of the mid-Ludfordian carbonates (for details see above) plotted together with the modeled 'response curves' for the marine δ^{44}Ca proxy based on hypothetical residence times (τ) of calcium in paleo-seawater of 20 000 and 1000 000 yrs. A horizontal axis (at the bottom) represents a relative time scale (in years), based on the reconstructed duration of the Mid-Ludfordian CIE using constraints from depositional rates and biostratigraphy (cf. Kozłowski and Sobień, 2012). Note that the scale for the $\delta^{44/40}$Ca-axis is reversed to enable changes in both Ca and C isotope systems to be more easily compared. (For interpretation of the references to color in this figure, the reader is referred to the web version of this article.)

in global seawater $\delta^{44/40}$Ca signatures over the same time frame as the change in seawater δ^{13}C values when the residence time of Ca in seawater is in excess of 1 million years (see the black curve in Fig. 3B). Theoretically, one could reproduce the observed $\delta^{44/40}$Ca trend in carbonates (blue circles; Fig. 3B), however, only with a much shorter and unrealistic residence time for Ca in the ocean of only about 20 000 yrs (the blue curve in Fig. 3B). This exercise thus clearly demonstrates that the observed synchronousness in the stratigraphic trends of $\delta^{44/40}$Ca and δ^{13}C in the upper part of the section (7 to 29 m) is not consistent with an 'open ocean' scenario, at least not for Ca isotopes. Hence, some other phenomena or processes must be invoked to explain this observation, such as (i) a local-scale elemental/sediment cycling involving mixing of isotopically distinct Ca sources (cf., Holmden et al., 2012a; Husson et al., 2015), and/or possible kinetic Ca isotope effects linked to changes in the rates of marine carbonate precipitation (Tang et al., 2008).

5.3. Evidence for 'kinetic' or rate-controlled Ca isotope effects during carbonate precipitation

To further evaluate whether *source mixing* or *kinetic effects* is the more plausible mechanism for explaining the observed $\delta^{44/40}$Ca

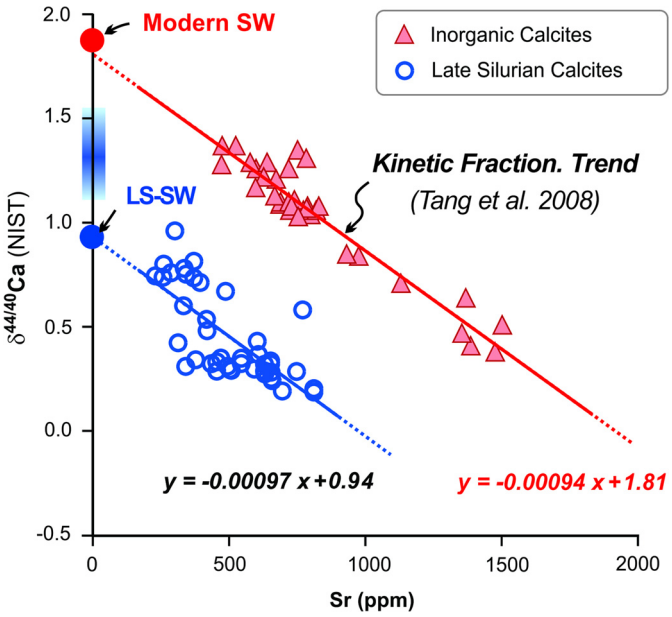

Fig. 4. The $\delta^{44/40}$Ca versus Sr content in carbonates, i.e., calcites, from this study (open blue circles = the mid-Ludfordian carbonates), and from the study of Tang et al. (2008) that investigated laboratory-controlled inorganic calcites (red triangles) formed under variable precipitation rates. Note that the latter data, and a solid red line (i.e., a kinetic fractionation trend), are both representative of a situation that assumes $\delta^{44/40}$Ca of a calcification fluid of 1.88‰ (i.e., as modern seawater, SW), which is illustrated as a red circle. A blue line represents a fitted 'trend line' through our data (i.e., open blue circles) that has a slope of -0.00097 ± 0.00016, which is within the error identical with the 'kinetic fractionation trend' of Tang et al. (2008) that has a slope of -0.00094. A solid blue circle represents an intercept of the 'trend line' based on our data, which according to the theory (cf., Tang et al., 2008) should also reflect the Ca isotope composition of the late Silurian seawater (LS-SW) in the Prague Basin. A vertical blue rectangle shows the estimated $\delta^{44/40}$Ca range of Silurian seawater based on data of globally distributed fossil brachiopods (Farkaš et al., 2007). (For interpretation of the references to color in this figure, the reader is referred to the web version of this article.)

variability in the mid-Ludfordian carbonates, we investigated the relationship between Ca isotopes and Sr concentrations in our profile (see Table 1A, Appendix). According to Tang et al. (2008), kinetic fractionation effects caused by variable rates of $CaCO_3$ precipitation should exhibit a linear trend between $\delta^{44/40}$Ca and Sr-concentrations, following the relationship:

$$\Delta^{44/40}\mathrm{Ca}_{\text{calcite-aq}} = -0.00094 * \mathrm{Sr}\ (\mathrm{ppm}) - 0.07 \pm 0.09 \qquad (4)$$

where $\Delta^{44/40}\mathrm{Ca}_{\text{calcite-aq}}$ is the isotope difference (in ‰) between the $\delta^{44/40}$Ca signature of precipitated calcite and that of a fluid (or seawater) from which the calcite is formed. It is noted that the precipitation rates ($\log R$) for the inorganic calcite experiments of Tang et al. (2008), ranging between 2–4 μmol/m^2/h, are comparable to rates for modern marine biogenic carbonates (e.g., calcitic foraminifera with $\log R$ of about 3 to 3.5; Kisakürek et al., 2011).

Plotting our data in the same coordinates ($\delta^{44/40}$Ca vs. Sr concentrations) as Tang et al. (2008) reveals a moderate yet statistically significant correlation between $\delta^{44/40}$Ca values and Sr concentrations ($r_s = -0.76$, $p < 0.001$, $n = 41$) and similar slope -0.00097 ± 0.00016 (see a blue line and open circles, Fig. 4). This co-variation between $\delta^{44/40}$Ca and Sr concentration data holds through the entire profile. According to Tang et al. (2008), the y-intercept should reflect the $\delta^{44/40}$Ca of a solution, i.e., paleo-seawater, if the $\delta^{44/40}$Ca values and Sr concentrations of the carbonates have not been altered during diagenesis. The y-intercept for the studied carbonates is $+0.94 \pm 0.08$‰ (a solid blue circle, Fig. 4), which is ~ 1‰ lower than the $\delta^{44/40}$Ca value of modern seawater (+1.86). This value ($+0.94 \pm 0.08$‰) is only slightly lower than published estimates of the early Paleozoic seawater based on fossil brachiopod data (Farkaš et al., 2007), which suggest $\delta^{44/40}$Ca values between +1.2 and 1.5‰ for late Silurian seawater (a blue vertical rectangle in Fig. 4, labeled as LS-SW = Late Silurian Seawater).

These estimates, however, involve assumptions that are difficult to quantify. Specifically, the paleo-seawater $\delta^{44/40}$Ca reconstructions based on fossil brachiopod data assume that the fractionation factor controlling the $\delta^{44/40}$Ca value of Silurian brachiopod calcite was the same as for modern species. Also, the y-intercept of the 'kinetic trend' acquired from marine sedimentary carbonates is susceptible to Sr-loss due to syndepositional or later diagenetic recrystallization. For example, if the degree of possible post-depositional Sr loss was relatively uniform among the studied carbonates in the profile, then the diagenetic process would cause the $\delta^{44/40}$Ca vs. Sr data trend to shift to the left on the diagram (Fig. 4), resulting in lower inferred seawater $\delta^{44/40}$Ca value (i.e., lower y-intercept), while possibly preserving the kinetic slope of the trend because $\delta^{44/40}$Ca is more resistant to alteration than Sr concentrations. On the other hand, the lower seawater $\delta^{44/40}$Ca values inferred from the y-intercept may be of *local* rather than *global* significance, due to input fluxes of Ca from local scale dissolution $CaCO_3$ sediment within the Prague Basin, including submarine and subaerial weathering of carbonate sediments and submarine groundwater discharge (Holmden et al., 2012a, 2012b).

Local-scale changes in the carbonate chemistry and $CaCO_3$ saturation state of seawater in the Prague Basin have the potential to drive such kinetically controlled variations in the studied carbonate $\delta^{44/40}$Ca record. These phenomena may include the recently suggested *carbonate hypersaturation* conditions of the mid-Ludfordian oceans, or local seawater in the Prague Basin, which should promote a rapid surficial degassing of CO_2 and CH_4 gases with a preferential loss of ^{12}C from the residual DIC pool. The consequence of such *kinetic isotope effects* linked to *carbonate hypersaturation* would be the precipitation of marine carbonates with heavy δ^{13}C and light $\delta^{44/40}$Ca values (cf., Kozłowski, 2015; Tang et al., 2008), in agreement with our observations (Fig. 1B, C).

5.4. Possible role of carbonate mineralogy: calcite vs. aragonite mixing

Ca isotope data from inorganic laboratory precipitation experiments, and from modern marine carbonates, indicate that calcite is often isotopically heavier than aragonite, by up to 0.6‰, due to differences in crystal lattice parameters and Ca–O bonding environments (Gussone et al., 2005). In addition, aragonite has also significantly higher Sr content compared to calcite (i.e., thousands vs. hundreds of ppm, respectively) and thus changes in the relative proportion of calcite vs. aragonite abundances in bulk carbonate sediments could generate a systematic coupling between stratigraphic changes in $\delta^{44/40}$Ca and Sr contents (cf. Husson et al., 2015). Such changes could be driven via (i) eustatically controlled migration of carbonate facies within a basin (e.g., mixing of deeper calcitic vs. shallower aragonitic sediments), and/or (ii) changes in the $CaCO_3$ mineralogy of the primary producers in the depositional setting.

Traditionally, the Silurian is considered to represent a stable period of typical 'calcitic seas' due to low marine Mg/Ca ratios (<2), (Mackenzie and Andersson, 2013). However, recent experimental studies suggest that it is not only the marine Mg/Ca ratio but also seawater temperature that controls the primary mineralogy of carbonate sediments (Balthasar and Cusack, 2015). Aragonite was likely a common constituent (>50%) of marine carbonate sediments even in the 'calcitic sea' of the late Silurian, if the temperature of seawater was >25 °C. It is therefore possible that the observed coupling between $\delta^{44/40}$Ca and Sr concentrations in the studied mid-Ludfordian carbonates (Fig. 4) could be due to mixing

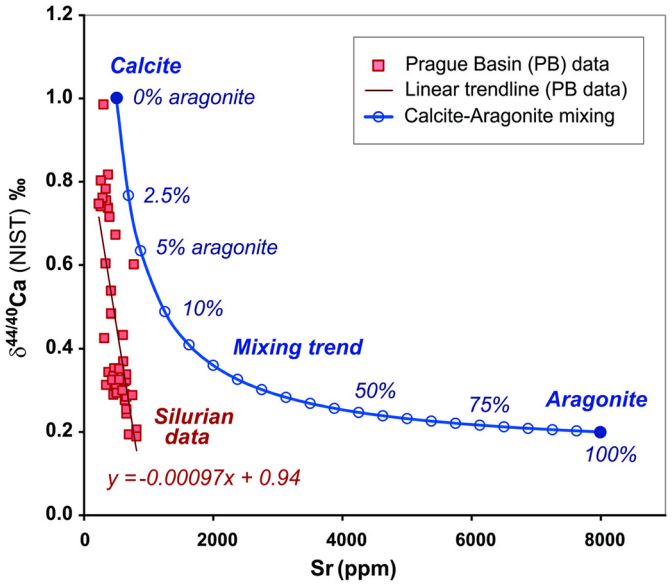

Fig. 5. The $\delta^{44/40}$Ca and Sr contents in modeled mixtures of pure *calcite* and *aragonite* end-members (calculated based on a mass balance approach, see Appendix, Table A3), and these are compared to $\delta^{44/40}$Ca and Sr data measured in the late Silurian (mid-Ludfordian) carbonates from the Prague Basin (i.e., red squares). Note that pure *calcite* end-member has $\delta^{44/40}$Ca of 1.0‰ and Sr concentration of 500 ppm, and *aragonite* has $\delta^{44/40}$Ca of 0.2‰ and Sr concentration of 8000 ppm. (For interpretation of the references to color in this figure, the reader is referred to the web version of this article.)

of sedimentary calcite and aragonite, rather than 'kinetic' isotope effects.

This alternative hypothesis is not without pitfalls that also require careful consideration. For example, the mixing of calcite and aragonite is not expected to generate a linear trend with the 'kinetic' slope of −0.000096 (as observed in our data) on the $\delta^{44/40}$Ca vs. Sr concentration diagram, but rather a hyperbolic trend (see Fig. 5). The degree of curvature of the mixing hyperbola is a function of the large difference in Sr concentration between aragonite and calcite. However, calcitization of the sediment during diagenesis will tend to linearize the mixing relation due to the loss of Sr from aragonite, bringing the Sr concentration of the secondary calcite closer to the Sr concentration of the primary calcite. However, if this is true, then slope of −0.000096, which is nearly in perfect agreement with the 'kinetic' slope determined from laboratory precipitation experiments (Tang et al., 2008), would have to be considered a coincidence. Alternatively, the 'kinetic' slope may be diagenetic feature produced during carbonate neomorphism rather than during carbonate precipitation in surface environments. However, carbonate precipitation rates should be low in diagenetic environments, presumably too low to produce the strong kinetic coupling between $\delta^{44/40}$Ca and Sr concentrations observed in our data and the experiments of Tang et al. (2008). In addition, mixing of sedimentary calcite and aragonite cannot by itself explain the extremely high δ^{13}C signatures (up to 8.5‰) recorded in the mid-Ludfordian carbonates, as aragonite is only about 1.8‰ higher in ^{13}C than calcite (Rubinson and Clayton, 1969). Finally, based on the new conodont δ^{18}O record of Trotter et al. (2016), paleo-seawater temperatures should be significantly (ca. 5 to 10 °C) *cooler* during the onset of the mid-Ludfordian CIE, and thus the conditions for aragonite precipitation should be less favorable during this time. Accordingly, one would expect to see higher $\delta^{44/40}$Ca values and lower Sr concentrations (due to less aragonite and more calcite in sediment) during this *cooler* interval at the onset of the CIE, which however is a prediction that is at odds with our data showing actually an opposite trend (see Figs. 1 and 4).

In summary, 'kinetic effects' likely did play an important role in establishing the range of the observed $\delta^{44/40}$Ca values in the studied mid-Ludfordian carbonates, but accepting this interpretation does not preclude the possibility that mineralogical effects may also be important. More research is needed to discern between these hypotheses for controlling carbonate $\delta^{44/40}$Ca values in marine carbonate successions, generally, and specifically during the mid-Ludfordian CIE being the largest positive δ^{13}C excursion of the entire Phanerozoic.

6. Conclusions

We investigated Ca isotope variability ($\delta^{44/40}$Ca) in late Silurian marine carbonates from the Prague Basin deposited during the mid-Ludfordian positive CIE. Our results show that during the onset of the CIE, when δ^{13}C increases from ~0‰ to ~8.5‰, $\delta^{44/40}$Ca remains constant at ~0.3‰, while ^{87}Sr/^{86}Sr data from least altered samples indicate a typical Ludfordian seawater composition. The absence of a coincident shift in $\delta^{44/40}$Ca in the beginning stages of the CIE is consistent with (i) the longer oceanic residence time of Ca compared to C, and (ii) the short duration of hypothesized glacio-eustatically driven sea level fluctuations on the order of ~10 000 yrs (cf., Kozłowski and Sobień, 2012).

Taking into account that our ^{87}Sr/^{86}Sr data from the least altered carbonates yielded typical Ludfordian seawater composition (with ^{87}Sr/^{86}Sr from ~0.70865 to ~0.70875), plausible processes for the origin of the mid-Ludfordian CIE include: (i) changes in oceanic circulation and stratification, i.e. the oceanic-climatic models (cf., Jeppsson, 1990; Bickert et al., 1997), (ii) near shore methanogenesis and intense photosynthesis (cf., Panchuk et al., 2006; LaPorte et al., 2009; Kozłowski and Sobień, 2012) associated with seawater *carbonate hypersaturation* in near shore settings (Kozłowski, 2015), and/or (iii) increase in the organic C production and burial in the global ocean (Kump and Arthur, 1999). The latter scenario (iii) is, however, not feasible considering the lack of evidence for increased organic carbon deposition in coeval marine sediments, and the fact that mass balance constraints indicate that the organic carbon burial flux in the global ocean would need to increase almost 3 times (from ~20% to ~55%) to generate the CIE with a magnitude of +8.5‰ and over such a short timescale.

Importantly, higher up in the profile (~10 to 30 m) where the positive CIE plateau is established and gradually declines back to 0‰ we observe a strong coupling between carbonate δ^{13}C and $\delta^{44/40}$Ca records (Fig. 1), with evidence for an overall 'kinetic' control of the observed Ca isotope variations (Fig. 4). The latter is indicated by a linear correlation between $\delta^{44/40}$Ca and Sr-concentration data ($r_s = -0.76$, $p < 0.001$, $n = 41$) with the 'kinetic' slope of −0.00097. The importance of kinetic processes, or rate controlled isotope effects, during the formation of the mid-Ludfordian CIE was recently suggested by Kozłowski (2015), and previously also by Holmden et al. (2012a) for the formation of the Hirnantian CIE. Both studies stressed the importance of (i) anomalous supplies of nutrients needed to drive increased local biological productivity in near shore regions of epeiric seas where the δ^{13}C excursions tend to be largest; and the associated (ii) increase in $CaCO_3$ saturation-state of local seawater that enables rapid carbonate precipitation. Kozłowski (2015) presented petrographic evidence for peculiar calcite 'sparoids' in peri-platform deposits recording the Ludfordian CIE in eastern Poland, which he interpreted to reflect calcite precipitation at the air-sea interface under conditions of locally enhanced *carbonate hypersaturation*. This is a scenario that is consistent with *kinetics* driving the variation in $\delta^{44/40}$Ca values in the study section, i.e., an increase in carbonate precipitation rate should correlate with a decrease in carbonate $\delta^{44/40}$Ca values. However, there is no corresponding (i.e., coeval) shift in $\delta^{44/40}$Ca values at the base of the CIE, suggesting that the

purported *carbonate hypersaturation* conditions of mid-Ludfordian seawater may have been present in the Prague Basin before the CIE. Higher up in the section, $\delta^{44/40}$Ca values increase at the same time that the CIE is declining to baseline values, which means that the hypothesized conditions of hypercalcification (i.e., *carbonate hypersaturation*) would also be declining. Here, the coupled Ca and C isotope changes support a decrease in carbonate precipitation rate. Alternatively, the change in $\delta^{44/40}$Ca values may reflect a shift in the mineralogy of the primary produced carbonate sediment from aragonite to calcite, reflecting a sea level driven change in carbonate depositional facies and carbonate polymorph mineralogy.

Future Ca isotope studies of late Silurian carbonates collected from different paleo-continents, and covering a wider range of paleo-environments, may shed more light on the question of whether *kinetics* or rather *carbonate mineralogy* represents the main control over the observed variations in $\delta^{44/40}$Ca record of mid-Ludfordian carbonates, and the cause of this largest positive CIE in Phanerozoic history.

Acknowledgements

This study was supported by the Czech Science Foundation via a GACR grant (P210/15-13310S), and partial support was also provided via the BASE-LiNE Earth project (No. 643084) funded by the European Commission within the Marie Sklodowska-Curie Actions under the Horizon 2020 program. We thank Jon Husson, Wojciech Kozłowski, and one anonymous reviewer, for their detail reviews and constructive comments that significantly improved the manuscript. Finally, an excellent editorial handling of Derek Vance is also acknowledged. This is a TRaX (Centre for Tectonics, Resources and Exploration, University of Adelaide) contribution No. 351.

Appendix A. Supplementary material

Supplementary material related to this article can be found online at http://dx.doi.org/10.1016/j.epsl.2016.06.038.

References

Balthasar, U., Cusack, M., 2015. Aragonite–calcite seas: quantifying the gray area. Geology 43, 99–102.

Banner, J., Hanson, G., 1990. Calculation of simultaneous isotopic and trace element variations during water–rock interactions with applications to carbonate diagenesis. Geochim. Cosmochim. Acta 54, 3123–3137.

Barrick, J.E., Kleffener, M.A., Gibson, M.A., Peavey, F.N., Karlsson, H.R., 2010. The mid-Ludfordian Lau Event and carbon isotope excursion (Ludlow, Silurian) in southern Laurentia – preliminary results. Boll. Soc. Paleontol. Ital. 49, 13–33.

Bickert, T., Pätzold, J., Samtleben, C., Munnecke, A., 1997. Palaeoenvironmental changes in the Silurian indicated by stable isotopes in brachiopod shells from Gotland, Sweden. Geochim. Cosmochim. Acta 61, 2717–2730.

Blättler, C.L., Henderson, G.M., Jenkyns, H.C., 2012. Explaining the Phanerozoic Ca isotope history of seawater. Geology 40, 843–846.

Brett, C.E., Ferreti, A., Histon, K., Schonlaub, H.P., 2009. Silurian sequence stratigraphy of the Carnic Alps, Austria. Palaeogeogr. Palaeoclimatol. Palaeoecol. 279, 1–28.

Calner, M., 2008. Silurian global events – at the tipping point of climate change. In: Ashraf, M.T. (Ed.), Mass Extinctions. Springer-Verlag, Berlin and Heidelberg, pp. 21–58.

Cramer, B.D., Munnecke, A., Scchofield, D.I., Haase, K.M., Haase-Schramm, A., 2011. A revised $^{87}Sr/^{86}Sr$ curve for the Silurian: implications for global ocean chemistry and the Silurian timescale. J. Geol. 119, 335–349.

Fanton, K.C., Holmden, C., 2007. Sea level forcing of carbon isotope excursions in epeiric seas: implications for carbon isotope chemostratigraphy. Can. J. Earth Sci. 44, 807–818.

Farkaš, J., Böhm, F., Wallmann, K., Blenkinsop, J., Eisenhauer, A., van Geldern, R., Munnecke, A., Voigt, S., Veizer, J., 2007. Calcium isotope record of Phanerozoic oceans: implications for chemical evolution of seawater and its causative mechanisms. Geochim. Cosmochim. Acta 71, 5117–5134.

Frýda, J., Frýdova, B., 2014. First evidence for the Homerian (late Wenlock, Silurian) positive carbon isotope excursion from peri-Gondwana: new data from the Barrandian (Perunica). Bull. Geosci. 89, 617–634.

Frýda, J., Frýdová, B., 2016. The Homerian (late Wenlock, Silurian) carbon isotope excursion from Perunica: does dolomite control the magnitude of the carbon isotope excursion? Can. J. Earth Sci. 53.

Frýda, J., Manda, Š., 2013. A long-lasting steady period of isotopically heavy carbon in the late Silurian ocean: evolution of the δ^{13}C record and its significance for an integrated δ^{13}C, graptolite and conodont stratigraphy. Bull. Geosci. 88, 463–482.

Gussone, N., Böhm, F., Eisenhauer, A., Dietzel, M., Heuser, A., Teichert, B.M.A., Reitner, J., Wörheide, G., Dullo, W.-Chr., 2005. Calcium isotope fractionation in calcite and aragonite. Geochim. Cosmochim. Acta 69, 4485–4494.

Holmden, C., Creaser, R.A., Muehlenbachs, K., Leslie, S.A., Bergstrom, S.M., 1998. Isotopic evidence for geochemical decoupling between ancient epeiric seas and bordering oceans. Implications for secular curves. Geology 26, 567–570.

Holmden, C., Panchuk, K., Finney, S.C., 2012a. Tightly coupled records of Ca and C isotope changes during the Hirnantian glaciation in an epeiric sea setting. Geochim. Cosmochim. Acta 98, 94–106.

Holmden, C., Papanastassiou, D.A., Blanchon, P., Evans, S., 2012b. $\delta^{44/40}$Ca variability in shallow water carbonates and the impact of submarine groundwater discharge on Ca-cycling in marine environments. Geochim. Cosmochim. Acta 83, 179–194.

Horita, J., Zimmermann, H., Holland, H.D., 2002. Chemical evolution of seawater during the Phanerozoic: implications from the record of marine evaporites. Geochim. Cosmochim. Acta 66, 3733–3756.

Husson, J.M., Higgins, J.A., Maloof, A.C., Schoene, B., 2015. Ca and Mg isotope constraints on the origin of Earth's deepest δ^{13}C excursion. Geochim. Cosmochim. Acta 160, 243–266.

Immenhauser, A., Della Porta, G., Kenter, J.A.M., Bahamonde, J.R., 2003. An alternative model for positive shifts in shallow-marine carbonate δ^{13}C and δ^{18}O. Sedimentology 50, 953–959.

Jeppsson, L., 1987. Lithological and conodont distributional evidence for episodes of anomalous oceanic conditions during the Silurian. In: Aldridge, R.J. (Ed.), Palaeobiology of Conodonts. Ellis Horwood, Chichester, West Sussex, pp. 129–145.

Jeppsson, L., 1990. An oceanic model for lithological and faunal changes tested on Silurian record. J. Geol. Soc. 147, 663–674.

Jeppsson, L., Talent, J.A., Mawson, R., Andrew, A., Corradini, C., Simpson, A.J., Wigfross-Lange, J., Schönlaub, A.P., 2012. Late Ludfordian correlation and the Lau Event, 653–675. In: Talent, J.A. (Ed.), Earth and Life, International Year of Planet Earth. Springer Science.

Kaljo, D., Kiipli, T., Martma, T., 1997. Carbon isotope event markers through the Wenlock–Pridoli sequence at Ohesaare (Estonia) and Priekule (Latvia). Palaeogeogr. Palaeoclimatol. Palaeoecol. 132, 211–223.

Kisakürek, B., Eisenhauer, A., Böhm, F., Hathorne, E.C., Erez, J., 2011. Controls on calcium isotope fractionation in cultured planktonic foraminifera, *Globigerinoides ruber* and *Globigerinella siphonifera*. Geochim. Cosmochim. Acta 75, 427–443.

Kozłowski, W., 2015. Eolian dust influx and massive whitings during the Kozlowski/Lau Event: carbonate hypersaturation as a possible driver of the mid-Ludfordian Carbon Isotope Excursion. Bull. Geosci. 90 (4), 807–840.

Kozłowski, W., Sobień, K., 2012. Mid-Ludfordian coeval carbon isotope, natural gamma ray and magnetic susceptibility excursions in the Mielnik IG-1 borehole. Palaeogeogr. Palaeoclimatol. Palaeoecol. 339, 74–97.

Kříž, J., 1991. The Silurian of the Prague Basin (Bohemia) – tectonic, eustatic and volcanic controls on facies and faunal development. Spec. Pap. Palaeontol. 44, 179–203.

Kump, L., Arthur, M.A., 1999. Interpreting carbon-isotope excursions: carbonates and organic matter. Chem. Geol. 161, 181–198.

Kump, L.R., Arthur, M.A., Patzkowsky, M.E., Gibbs, M.T., Pinkus, M.T., Sheehan, P.M., 1999. A weathering hypothesis for glaciation at high atmospheric pCO_2 during the Late Ordovician. Palaeogeogr. Palaeoclimatol. Palaeoecol. 152, 173–187.

LaPorte, D.F., Holmden, C., Patterson, W.P., Loxton, J.D., Melchin, M.J., Mitchell, C., Finney, S.C., Sheets, H.D., 2009. Local and global perspectives on carbon and nitrogen cycling during the Hirnantian Glaciation. Palaeogeogr. Palaeoclimatol. Palaeoecol. 276, 182–195.

Lehn, G.O., Jacobson, A.D., Holmden, C., 2013. Precise analysis of Ca isotope ratios ($\delta^{44/40}$Ca) using an optimized ^{43}Ca–^{42}Ca double-spike MC-TIMS method. Int. J. Mass Spectrom. 351, 69–75.

Lehnert, O., Eriksson, M.J., Calner, M., Joachimski, M., Buggisch, W., 2007a. Concurrent sedimentary and isotopic indications for global climatic cooling in the Late Silurian. Acta Palaeontol. Sin. 46, 249–255.

Lehnert, O., Frýda, J., Buggish, W., Munnecke, A., Nützel, A., Kříž, J., Manda, Š., 2007b. δ^{13}C Record across the Ludlow Lau event: new data from mid palaeo-latitudes of northern peri-Gondwana (Prague Basin, Czech Republic). Palaeogeogr. Palaeoclimatol. Palaeoecol. 245, 227–244.

Loydell, D.K., 2007. Early Silurian positive δ^{13}C excursions and their relationship to glaciations, sea-level changes and extinction events. Geol. J. 42, 531–546.

Loydell, D.K., Frýda, J., 2011. At what stratigraphical level is the mid Ludfordian (Ludlow, Silurian) positive carbon isotope excursion in the type Ludlow area, Shropshire, England? Bull. Geosci. 83, 197–208.

Mackenzie, F.T., Andersson, A.J., 2013. The marine carbon system and ocean acidification during Phanerozoic time. Geochem. Perspect. 2, 227.

Manda, Š., Štorch, P., Slavík, L., Frýda, J., Kříž, J., Tasáryová, Z., 2012. Graptolite, conodont and sedimentary record through the late Ludlow Kozlowski Event (Silurian) in shale dominated succession of Bohemia. Geol. Mag. 149, 507–531.

Melchin, M.J., Holmden, C., 2006. Carbon isotope chemostratigraphy in Arctic Canada. Seal-level forcing of carbonate platform weathering and implications for Hirnantian global correlation. Palaeogeogr. Palaeoclimatol. Palaeoecol. 234, 186–200.

Munnecke, A., Samtleben, C., Bickert, T., 2003. The Ireviken Event in the lower Silurian of Gotland, Sweden – relation to similar Palaeozoic and Proterozoic events. Palaeogeogr. Palaeoclimatol. Palaeoecol. 195, 99–124.

Panchuk, K.M., Holmden, C., Leslie, S.A., 2006. Local controls on carbon cycling in the Ordovician Midcontinent region of North America with implications for carbon isotope secular curves. J. Sediment. Res. 76, 200–211.

Rubinson, M., Clayton, R.N., 1969. Carbon-13 fractionation between aragonite and calcite. Geochim. Cosmochim. Acta 33, 997–1002.

Schrag, D.P., Higgins, J.A., Macdonald, F.A., Johnston, D.T., 2013. Authigenic carbonate and the history of the global carbon cycle. Science 339, 540–543.

Swart, P.K., 2008. Global synchronous changes in the carbon isotopic composition of carbonate sediments unrelated to changes in the global carbon cycle. Proc. Natl. Acad. Sci. 105, 13741–13745.

Swart, P.K., Kennedy, M.J., 2011. Does the global stratigraphic reproducibility of $\delta^{13}C$ in Neoproterozoic carbonates require a marine origin? A Pliocene–Pleistocene comparison. Geology 40, 87–90.

Talent, J.A., Mawson, R., Andrew, A.S., Hamilton, P.J., Whitford, D.J., 1993. Middle Palaeozoic extinction events: faunal and isotopic data. Palaeogeogr. Palaeoclimatol. Palaeoecol. 104, 139–152.

Tang, J., Dietzel, M., Böhm, F., Köhler, S.J., Eisenhauer, A., 2008. Sr^{2+}/Ca^{2+} and $^{44}Ca/^{40}Ca$ fractionation during inorganic calcite formation: II. Ca isotopes. Geochim. Cosmochim. Acta 2008 (72), 3733–3745.

Torsvik, T.H., 2009. BugPlates: linking biogeography and palaeogeography. Available from http://www.geodynamics.no?bugs?SoftwareManual.pdf.

Trotter, J.A., Williams, I.S., Barnes, Ch.R., Männik, P., Simpson, A., 2016. New conodont $\delta^{18}O$ records of Silurian climate change: implications for environmental and biological events. Palaeogeogr. Palaeoclimatol. Palaeoecol. 443, 34–48.

Urbanek, A., Teller, L., 1997. Graptolites and stratigraphy of Wenlock and Ludlow Series in the East European platform. In: Urbanek, A., Teller, L. (Eds.), Silurian Graptolite Faunas of the East European Platform: Stratigraphy and Evolution. In: Palaeontologia Polonica, vol. 56, pp. 87–231.